

In-situ observation of coupled growth morphologies in organic peritectics

This article has been downloaded from IOPscience. Please scroll down to see the full text article.

2012 IOP Conf. Ser.: Mater. Sci. Eng. 27 012028

(<http://iopscience.iop.org/1757-899X/27/1/012028>)

View [the table of contents for this issue](#), or go to the [journal homepage](#) for more

Download details:

IP Address: 178.191.204.136

The article was downloaded on 31/05/2013 at 10:08

Please note that [terms and conditions apply](#).

In-situ observation of coupled growth morphologies in organic peritectics

J P Mogeritsch and A Ludwig

Chair of Simulation and Modelling of Metallurgical Processes,
University of Leoben, Franz-Josef-Str. 18, A-8700 Leoben, Austria

Email: mogeritsch@unileoben.ac.at

Abstract. Systematic directional solidification experiments were done with TRIS-NPG organic peritectic alloys to investigate peritectic solidification close to the limit of constitution undercooling. The experiments were carried out as in-situ observation in a horizontal micro Bridgman furnace. Under specific conditions isothermal peritectic coupled growth (PCG) were obtained for alloys within the hypo-peritectic region. Isothermal PCG was obtained either by (i) reducing the growth velocity from above the critical value for morphological stability of both solid phases to a value below, or by (ii) long-time growing with a constant velocity below the critical value for morphological stability of both solid phases. The later happens via island banding, where nucleation and lateral growth of the peritectic phase compete with growth of the primary phase. Interphase spacings and the widths of α and β lamellae were measured as function of growth velocity for a fixed composition and as function of composition for a fix growth velocity.

1. Introduction

It has become obvious from investigations of directional solidified peritectic alloys (Zn–Ag [1], Sn–Cd [2-5], Cu–Sn [6], Pb–Bi [7-11], Zn–Cu [12-14], Sn–Sb [15-16], Ti–Al [17-18], Fe–Ni [19-28], Ni–Al [29], YBCO [30], Nd–Fe–B [31] and TRIS–NPG [32-34]) that peritectic systems show a variety of complex microstructures. Close or below the limit of constitutional undercooling of both solid phases isothermal peritectic coupled growth (PCG), cellular peritectic coupled growth, discrete bands, island bands, and oscillatory tree-like structures were found [35-38]. It is especially the observation of two-phase growth, either coupled or banded, which has drawn the recent attention of researchers to this field [18, 20, 21, 24, 29, 39, 40].

In the present work, the organic non-faceted/non-faceted (nf/nf) peritectic system TRIS (Tris-(hydroxylmethyl)aminomethane)–NPG (Neopentylglycol) [41] is used as a model substance for metallic solidification by performing in-situ observations of peritectic solidification morphologies which occur close to the critical value for morphological stability [32-34]. Both organic substances show a low temperature faceted phase and a transparent non-faceted high temperature phase, which forms in an intermediate concentration range of the peritectic equilibrium, see Figure 1. The circumstance of having a nf/nf peritectic equilibrium in a transparent organic system enables in-situ observations of peritectic solidification pattern in a horizontal micro Bridgman furnace.

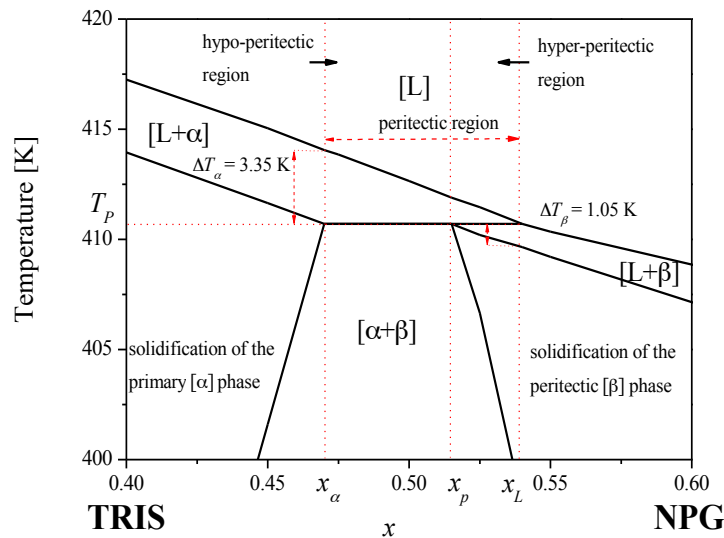


Figure 1: Detail of a peritectic phase diagram. At the peritectic temperature T_p and the peritectic concentration C_p the α , β and liquid phase are in equilibrium. The peritectic composition range x_α to x_L divided in to the hypo-peritectic range from x_α to x_p and the hyper-peritectic range from x_p to x_L . At concentrations $x_0 < x_\alpha$, only the α phase is in equilibrium with the liquid and for $x_0 > x_L$ only the β phase.

2. Experimental procedure

The organic substances NPG and TRIS were obtained from Aldrich [42] with an indicated purity of 99% and 99.9+ %, respectively. Both compounds were dehydrated in inert atmosphere at 310 K for 24 hours. For the preparation of the different initial alloy compositions the pure substances were weighed, joined, and heated in small glass containers. Different types of sample geometries and sealing substances/procedures were tested. Due to the relatively high hot zone temperature necessary for peritectic solidification experiments, many sealing materials tested such as UV hardening and silica-based glues, started leaking after some hours. The best results were obtained using large rectangle tubes (2000 μm x 100 μm inner diameter and 100 μm wall thickness [43]) with glued ends.

The alloy and sample preparation was performed within an Argon-filled glove box. The humidity within the glove box was reduced to below 10^4 ppm and the oxygen content below $2 \cdot 10^3$ ppm, estimated with a hygrometer and an air oxygen measuring device. For the preparation of the different alloy compositions the pure substances were weighed and joined in small glass containers, which were closed with plastic caps afterwards. Next, the glass container was heated on a hot plate until the organic powder melted, then it was shaken to improve the mixing, and then slowly solidified (~ 1 hour). This procedure lead to a refining of the alloys because impurities with a boiling temperature lower than the organic powder (e.g. water) should have condensed on the cap of the glass container. A similar refining procedure of the hygroscopic NPG was reported by Barrio et al. [41]. When the alloy was fully solidified, the glass container was crushed, and the waxen alloy was ground and filled into a new storage container. From this container small amounts of the alloy were taken to fill the rectangle glass tubes.

For the filling, the rectangular glass tubes were laid on a hot plate, in such a way that one side was on the plate and the other side protruded freely. Small amounts of the alloy were deposited on the hot plate next to the open side of the tube. As soon as the alloy melted, the liquid was dragged into the tube by capillarity until it reached the colder side of the tube where it solidified. This procedure ensured that enough room for expansion due to melting (and heating) was left free. Next, the tube was slowly dragged off the hot plate allowing the material to solidify and then both ends were sealed. During the investigations in the Bridgman furnace, both ends of the tubes were outside of the Bridgman furnace, and kept around room temperature, to let the solid alloy further seal the liquid part of the tube.

The horizontal micro Bridgman furnace consists of a cold and a hot copper block with 4 mm adiabatic gap, described in details in [44]. The hot zone block was heated to 453 K using heating wire; the cold zone temperature was controlled by a water circuit and set to 353 K. The temperatures on both sides were measured with Pt 100 temperature sensors placed inside the copper blocks and regulated independently with an accuracy of ± 0.1 K. The selected process conditions gives a linear temperature gradients $G = 14.2$ K/mm. The microscope was equipped with a CCD camera and self-developed software allowing the recording and storage of images, and temperature data. Samples with an extra large ratio rectangle tube (100 μm x 2000 μm inner diameter and 100 μm wall thickness [43]) were used to ensure a minimum of convection. The samples were filled with the organic alloys by capillary forces.

The solidification morphologies of the solid/liquid interface were investigated at selected pulling rates, V , and with a fixed temperature gradient G ($1.4 \cdot 10^4$ K/m). Preliminary studies of the physical parameters have revealed a diffusion coefficient D of $2.0 \cdot 10^{-11} \pm 0.6 \cdot 10^{-11}$ K/m within the peritectic region. During the solidification process pictures of the solid/liquid interface were taken every 30 seconds. Note that with a typical growth velocity of 0.1 $\mu\text{m/s}$ it took to more that 11 hours to solidify a length of about 4 mm. Due to such the long experimental runs most of the exiting findings presented in this paper were done by evaluation the huge amount of recorded pictures.

3. Results and discussion

In order to get an isothermal PCG we have used different hypo-peritectic alloys ($x_a < x_0 < x_b$), and different growth velocities. The temperature gradient was kept constant. As a matter of fact, we were able to achieve the isothermal PCG under two different conditions: (i) by long-time growing with a constant velocity below the critical value for morphological stability of both solid phases that's via island bands, and (ii) reducing the growth velocity from above the critical value for morphological stability of both solid phases to a value below.

Isothermal PCG by competition between lateral growth and nucleation via island bands

A hypo-peritectic sample with $x_0 = 0.51$ mol fraction NPG at a pulling rate $V = 0.19$ $\mu\text{m/s}$ shows a transformation from discrete bands via island bands to isothermal PCG. The transition from island bands to isothermal PCG is shown in figure 2. Although optically indistinguishable the two different solid phases can indirectly be differentiated by experiences based on phase diagram information, on several observations for different alloy concentrations, growth velocities, and on careful observations of the dynamic of changes. Our in-situ study of the transformation from discrete bands to isothermal PCG starts by an overgrowth of a planar L/ α interface by the peritectic β phase. The planar β solidification front grows stable till the primary α phase nucleates again at various positions at the L/ β interface. Now the lateral growth of α competes with the forward growth of β . During this competition β also nucleate on various positions at the L/ α interface happens. This situation is known as the stage of island bands (see figure 2c) [23]. With a suitable nucleation frequency, an adequate ratio of lateral, and forward growth of the two solid phases isothermal PCG establishes within around 20 minutes (figure 2d). Corresponding to the position of the alloy concentration within the peritectic plateau ($x_a = 0.47$ mol fraction $< x_0 = 0.51$ mol fraction $< x_b = 0.515$ mol fraction) the width of the β lamellae, λ_β , is large, and that of the α lamellae, λ_α , is small. Note that in the frame of the present optical resolution the interface seems to be strictly isothermal grow.

Isothermal PCG by reducing the growth velocity

In our experiments, different from what has been reported in literature so far, isothermal PCG could also be achieved by reducing the growth velocity from above the critical value for morphological stability of both solid phases to a value below. The formation of isothermal PCG for a hypo-peritectic alloy with $x_0 = 0.5$ mol fraction NPG by reducing the growth velocity from $V = 0.64$ $\mu\text{m/s}$ down to $V = 0.19$ $\mu\text{m/s}$ starts from simultaneous growth of an array of α dendrites ahead of an array of β cells. Figure 3a shows that the array of α dendrites and the array of β cells grow at different depth in the sample, whereby the peritectic β phase grows 0.8 ± 0.3 K behind the primary α phase. By reducing the growth velocity the two arrays tend to form two separate disturbed solid/liquid interfaces, L/ α in the background and L/ β in the front (Figure 3c). As the two interfaces get closer and closer to planarity they start to interact with each other. By careful studying the corresponding video sequence it becomes

obvious that the α phase starts to form islands at the L/ β interface, which then transform into α lamellae, which grow isothermal side-by-side with β lamellae (Figure 3d).

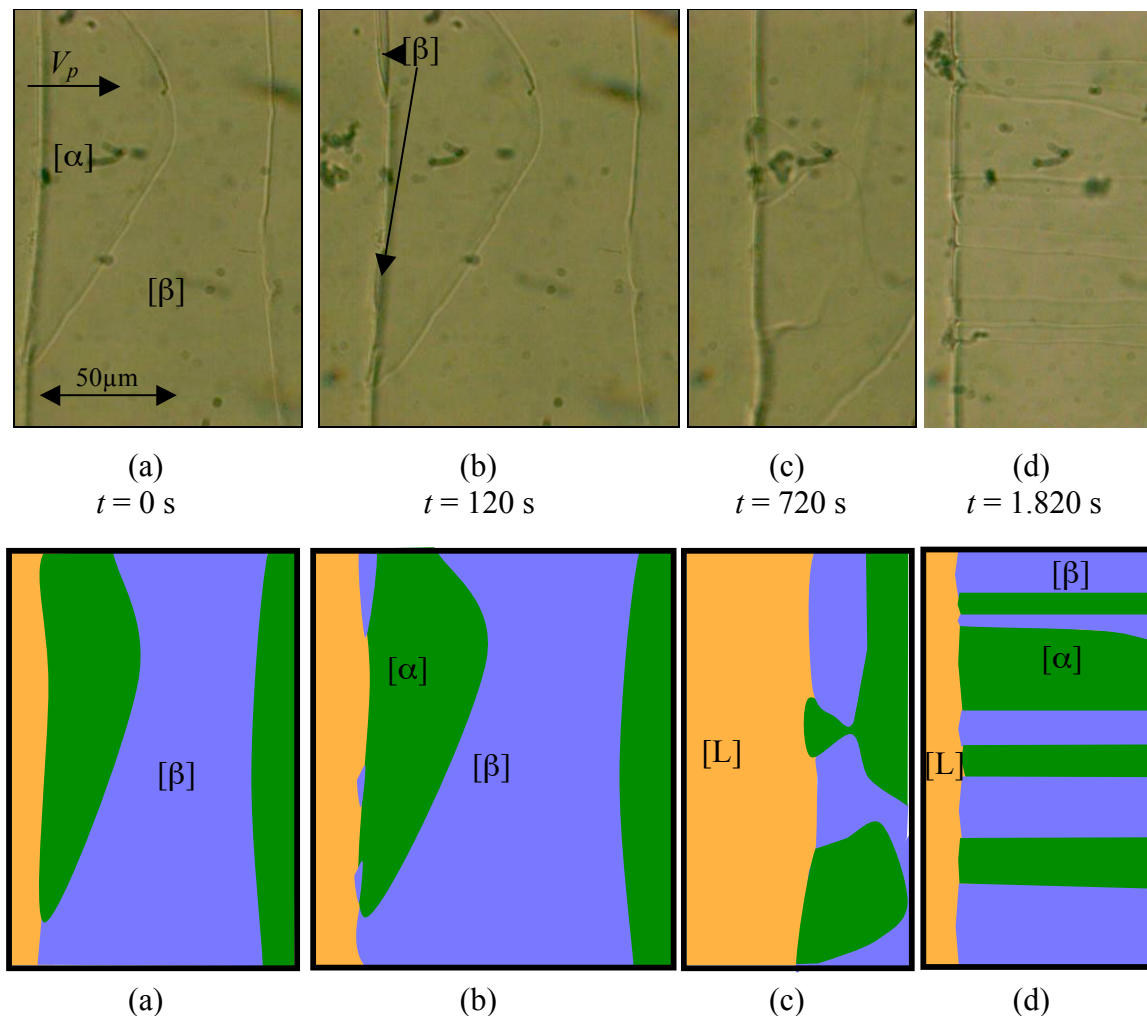


Figure 2. Initiation of PCG from island banding. Successive nucleation and growth of α and β in form of island bands leads to the formation of isothermal PCG. The observation was made for an hypo-peritectic alloy with $x_0 = 0.51$ mol fraction NPG and a pulling velocity of $V = 0.19 \mu\text{m/s}$.

Interphase spacing and width of the α and β lamellae

In most cases the α and β lamellae, which occur during isothermal PCG, were parallel and straight. Only in a few cases, short wavelength oscillatory instabilities, which are reminiscent of $1 - \lambda$ instabilities, occur. However, no systematical studies on this topic were made so far.

Although the optical impression on the width of a lamella depends to some extent on the focus depth of the microscope, the width of the α and β lamellae as well as the interphase spacing has been estimated in an averaged way for different moments in time and at different positions. In figure 4 the interphase spacing and width of α and β lamellae are shown as function of growth velocity for a hypo-peritectic concentration $x_0 = 0.5$ mole fraction NPG. From eutectic solidification it is known that the interphase spacing increasing with decreasing growth velocity. Our measurements suggest that this might be different for peritectic solidification. Although the error bar at $V = 0.07 \mu\text{m/s}$ is quite large the decrease of λ for smaller growth velocity seems significant. In figure 4 the interphase spacing and width of α and β lamellae are shown as function of concentration for $V = 0.19 \mu\text{m/s}$. Obviously, the interphase spacing reveals a minimum at the concentration of around $x_0 = 0.5$ mol fraction NPG.

Finally, it is worth mentioning that the ratio of lamella width to interphase spacing is in good agreement with the position of x_0 within the peritectic interval ($x_\beta - x_\alpha$).

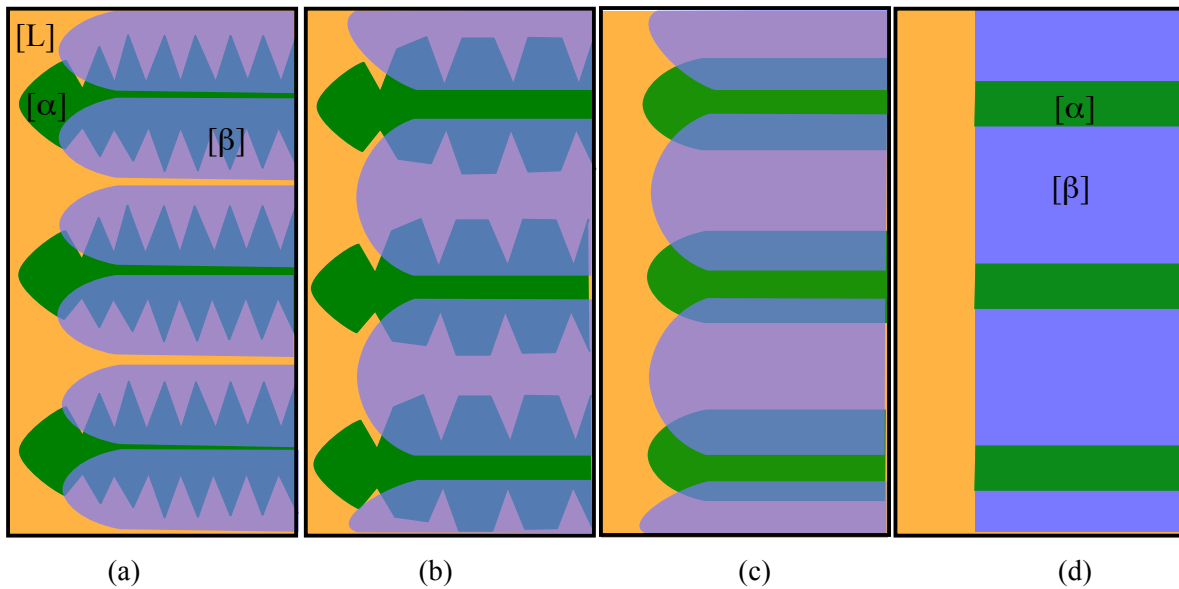


Figure 3. Development of isothermal PCG by reducing the growth velocity from $V = 0.64 \mu\text{m/s}$ down to $V = 0.19 \mu\text{m/s}$ for a hypo-peritectic alloy with $x_0 = 0.5$ mol fraction NPG. The transition from a dendritic/cellular interface to isothermal PCG took around 900 s. As initial state an array of α dendrites grew ahead (and behind) of an array of β cells.

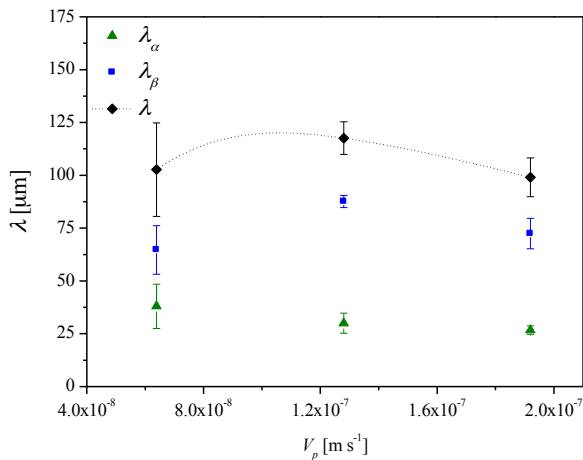


Figure 4. Measured averaged interphase spacing, λ , and width of α and β lamellae, λ_α and λ_β , as function of growth velocity for $x_0 = 0.50$ mol fraction NPG.

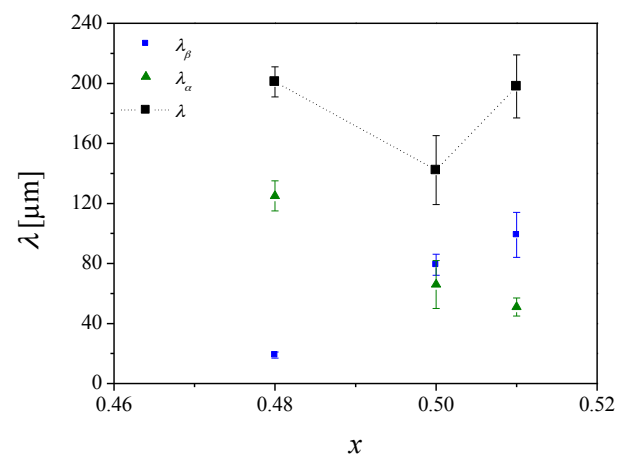


Figure 5. Measured averaged interphase spacing, λ , and width of α and β lamellae, λ_α and λ_β , as function of concentration for a growth velocity $V = 0.19 \mu\text{m/s}$.

4. Conclusions

As presented in this work, direct in-situ observations of the formation of isothermal PCG were possible by using a transparent nf/nf peritectic alloy. We found that isothermal PCG can be obtained by two different ways: (i) by long-time growing with a constant velocity below the critical value for morphological stability of both solid phases that's via island bands, and (ii) reducing the growth velocity from above the critical value for morphological stability of both solid phases to a value below. For both cases observations on the dynamic of the formation of isothermal PCG is given. The ratio of lamella width to interphase spacing, predicted by the level rule, is in good agreement with the position of x_0 within the peritectic interval. However, we have presented experimental results that suggest that the interphase spacing in isothermal PCG might reveal a maximum at a certain growth velocity rather than increasing further with decreasing velocity.

Acknowledgement

This research has been supported by the Austrian Research promotion Agency (FFG) in the frame of the METTRANS project and by the European Space Agency (ESA) in the frame of the METCOMP project.

References

- [1] Uhlmann DR and Chadwick GA, 1961 *Acta Metall.* **9** 835–840.
- [2] Boettinger WJ, 1974 *Metall. Trans.* **5** 2023–2031.
- [3] Trivedi R and Park J S, 2002 *J. Cryst. Growth* **235** 572–588.
- [4] Trivedi R and Shin JH, 2005 *Mater. Sci. Eng. A* **413–414** 288–295.
- [5] Yasuda H, Notake N, Tokieda K and Ohnaka I, 2000 *J. Cryst. Growth* **210** 637–645.
- [6] Kohler F, Germond L, Wagnière JD and Rappaz M, 2000 *Acta Mater.* **57** 56–68.
- [7] Karma A, Rappel W J, Fuh B C and Trivedi R, 1998 *Metall. Trans. A* **29** 1457–1470.
- [8] Tokieda K, Yasuda H and Ohnaka I, 1999 *Mater. Sci. Eng. A* **262** 238–245.
- [9] Lograsso T A, Fuh B C and Trivedi R, 2005 *Metall. Trans. A* **36** 1287–1300.
- [10] Liu S and Trivedi R, 2006 *Metall. Trans. A* **37** 3293–3304.
- [11] Hu XW, Li SM, Chen WJ, Gao SF, Liu L. and Fu HZ, 2009 *J. Alloys Comp.* **484** 1631–636.
- [12] Ma D, Li Y, Ng SC and Jones H, 2000 *Acta Mater.* **48** 1741–1751.
- [13] Ma D, Li Y, Ng SC and Jones H, 2000 *Acta Mater.* **48** 419–431.
- [14] Li Y, Ng SC and Jones H, 1998 *Scripta Mater.* **39** 7–11.
- [15] Hu XW, Li S M, Liu L and Fu HZ, 2008 *China Foundry* **5** 167–171.
- [16] Titchener AP, Spittle JA, 1975 *Acta Metall.* **23** 497–502.
- [17] Su Y Q, Liu C, Li XZ, Guo JJ, Li BS, Jia J and Fu HZ, 2005 *Intermetallics* **13** 267–274.
- [18] Busse P and Meissen F, 1997 *Scripta Mater.* **36** 653–658.
- [19] Luo LS, Su YQ, Guo JJ, Li XZ, Li SM, Zhong H, Liu L and Fu HZ, 2008 *J. Alloys Comp.* **461** 121–127.
- [20] Su YQ, Luo LS, Li XZ, Guo JJ, Yang HM and Fu HZ, 2006 *Appl. Phys. Lett.* **89** 2319181–2319183.
- [21] Luo LS, Su Y Q, Li XZ, Guo JJ, Yang HM and Fu HZ, 2008 *Appl. Phys. Lett.* **92** 0619031–0619033.
- [22] Vandyoussefi M, Kerr HW and Kurz W, 2000 *Acta Mater.* **48** 2297–2306.
- [23] Lo TS, Dobler S, Plapp M, Karma A and Kurz W, 2003 *Acta Mater.* **51** 599–611.
- [24] Dobler S, Lo T S, Plapp M, Karma A and Kurz W, 2004 *Acta Mater.* **52** 2795–2808.
- [25] Massaki Sumida, 2003 *J. Alloys Comp.* **349** 302–310.
- [26] Feng Z, Shen J, Min Z, Wang L and Fu H, 2010 *Mater. Lett.* **64** 1813–1815.
- [27] Vandyoussefi M, Kerr HW and Kurz W, 1997 *Acta Mater.* **45** 4093–4105.
- [28] Luo LS, Su YQ, Guo JJ, Li XZ and Fu HZ, 2007 *Sci China Phys Mech. Astron.* **50** 442–450.
- [29] Lee JH and Verhoeven JD, 1994 *J. Cryst. Growth* **144** 353–366.
- [30] Rao QL, Fan XL, Shu D and Wu CC, 2008 *J. Alloys Comp.* **461** L29–L33.
- [31] Zhong H, Li SM, Lü HY, Liu L, Zou GR and Fu HZ, *J. Cryst. Growth* 2008 **310** 3366–3371.
- [32] Mogeritsch J, Ludwig A, Eck S, Grasser M and McKay B, 2009 *Scripta Mater.* **60** 882–885
- [33] Mogeritsch J, Eck S, Grasser M and Ludwig A, 2009 *Mater. Sci. Forum* **649** 159–64
- [34] Ludwig A, Mogeritsch J and Grasser M, 2009 *Trans. Indian Inst. Metals* **62** 433–436
- [35] Kerr HW, Kurz W, 1996 *Int. Mater. Rev.* **41** 129–164.
- [36] Luo W, Shen J, Min Z and Fu H, 2008 *J. Cryst. Growth* **24** 5441–6.
- [37] Hunziker O, Vandyoussefi M and Kurz W, 1998 *Acta Mater.* **18** 6325–6336.
- [38] Luo WZ, Shen J, Min ZX and Fu HZ, 2009 *Mater. Lett.* **63** 1419–21.
- [39] Li Y, Ng SC and Jones H, 1998 *Scripta Mater.* **39** 7–11.
- [40] Luo LS, Su Y Q, Guo JJ, Li X Z, Li SM, Zhong H, Liu L and Fu HZ, 2008 *J. Alloys Comp.* **461** 121–127.
- [41] Barrio M., Lopez DO., Tamarit JL., Negrier P. and Haget Y., 1995 *J. Mater. Chem.* **5** 431–437.
- [42] <http://www.sigmadrich.com>
- [43] <http://fscimage.fishersci.com> search for 126-30-7 and 77-86-1
- [44] Mogeritsch J, 2011 Ph.D. Thesis, University of Leoben